Model Based In Situ Calibration of Six Axis Force Torque Sensors

Francisco Javier Andrade Chavez[1,2], Silvio Traversaro[2], Daniele Pucci[2] and Francesco Nori[2]

Abstract— This paper proposes and validates an *in situ* calibration method to calibrate six axis force torque (F/T) sensors once they are mounted on the system. This procedure takes advantage of the knowledge of the model of the robot to generate the expected wrenches of the sensors during some arbitrary motions. It then uses this information to train and validate new calibration matrices, taking into account the calibration matrix obtained with a classical Workbench calibration. The proposed calibration algorithm is validated on the F/T sensors mounted on the iCub humanoid robot legs.

I. INTRODUCTION

Six axis force torque (F/T) sensors have been used in robotics systems since the 1970's [1]. Around the same time research on force control began [2]. F/T sensing has become a important sensing capability which can be highly exploited in robotics since is an essential knowledge for regulating contact forces and torques. Although strain gauge-based sensing technology has been widely used in industrial robots, its practical use in humanoids robots have been limited by the experimental evidence that installing the F/T sensors into complex structures such as Humanoids seems to change the measurements returned by the sensors making them unreliable. As explained in [3], during the last DARPA Robotics Challenge most of the teams could not take advantage of having such sensors. The Boston Dynamics ATLAS' Six Axis F/T sensors were not used due to the bad quality of sensors measurements, to the point that the IHMC and MIT teams used the F/T sensors only as binary contact sensor. In standard operating conditions, relevant changes in the calibration matrix may occur in months. F/T sensors are recommended to be calibrated at least once a year as stated by ATI [4] and Weiss Robotics [5] which are some of the leading companies for F/T sensors. The calibration procedure is done by the manufacturer company which implies that the sensor must be unmounted and sent back to them and then mounted again. It has been noted during different experiments that the reliability of the measurements changes after mounting the sensor on the robot, even in recently calibrated sensors. The knowledge of external forces on the robot can be used for more advanced control strategies, which makes

having a properly calibrated F/T sensor essential for allowing robots to perform more complex actions.

Most of the six axis F/T sensors available on the market are based on silicon or metallic strain gauges technologies, even if alternative technologies are starting to be adopted [6].

The commonly used model for predicting the force-torque from the raw strain gauges measurements of the sensor is an affine model. This model is sufficiently accurate since these sensors are mechanically designed and mounted so that the strain deformation is (locally) linear with respect to the applied forces and torques. Then, the calibration of the sensor aims at determining the two components of this model, i.e. a six-by-six matrix and a six element vector. These two components are usually referred to as the sensor's *calibration matrix* and *offset*, respectively. Preponderant changes in the sensor's offset can occur in hours, however, and this in general requires to estimate the offset before using the sensor.

The typical calibration procedure considers first identifying the offset when no load is applied on the sensor and then carefully place some weights in specific positions to have well known gravitational forces and torques in order to span the space of the sensor. The methods for obtaining the calibration matrix have been thoroughly studied and, although many methods exist, least squares remains the most popular [7]. For simplifying the time consuming procedure of careful load placing some specialized structures have been designed [8], [1]. In other cases a previously calibrated sensor is used as reference [9] [10]. This has the disadvantage of depending on the availability of another sensor which is not always the case.

The difference that has been observed on a six axis F/T sensor after being mounted has motivated the search for *in situ* calibration methods [11]. Among other advantages, these methods allow to perform the calibration in the sensor's final destination avoiding possible modification of the calibration matrix that arise from mounting and removing the sensors from its working structure. To the best of our knowledge, the first *in situ* calibration method for force-torque sensors was proposed in [12]. But this method exploits the topology of a specific kind of manipulators, which are equipped with joint torque sensors then leveraged during the estimation. Another in situ calibration technique for force-torque sensors can be found in [13]. But the use of supplementary already-calibrated force-torque/pressure sensors impairs this technique for the reasons we have discussed before.

In our previous work [11] a F/T sensor was calibrated *in situ* by assuming that a single rigid body equipped with an accelerometer was attached to the F/T sensor. While we assumed that the inertial parameters (mass, center of mass,

Fig. 1: Location of the six axis F/T sensors mounted on the iCub. The F/T sensors are embedded in the robot structure rather then being mounted only on the end/effectors to estimate the joint torques, as explained in [14].

3D inertia tensor) of the attached rigid body were unknown, nevertheless we assumed that a set of additional masses of known mass was attached to the F/T sensor load in the various experiments. Even the (limited) assumptions of [11] complicated a lot the use of the introduced techniques. In particular the need for knowing a-priori the accelerometer orientation w.r.t. the F/T sensor frame and the assumption that only a rigid body was attached to the F/T sensor complicated the use of such techniques in the case of F/T embedded in the robot structure for performing joint torques estimation [14]. To overcome this limitations, in this paper we assume that the inertial parameters of robot links are known. While this may seem a rather bold assumption, it is possible if the inertial parameters obtained from the Computer Aided Manufacturing (CAD) model of the robot are validated by weighting experiments on the individual robot links, as was our case.

There are two main contribution in this paper. The first one is to formulate the calibration problem by decoupling the offset estimation problem from the calibration matrix estimation problem, enabling the use of multiple datasets with multiple unknown offsets that share the same calibration matrix. The second one is to cast the calibration matrix estimation problem as *regularized least square* problem, in which the regularization takes into account the information known from a previous available calibration matrix.

The proposed algorithms are validated by calibrating a six axis F/T sensor found in the right leg of an iCub humanoid robot. Some of the calibration and validation datasets come from real world scenarios in which the iCub is switching from two feet balancing to one foot balancing.

The paper is organized as follows. Section II-B describes the formulation of the problem. Section III describes the strategies used to do the *model based in situ* calibration. Section IV describes the characteristics of the datasets used for training and the validation procedures used. Section V shows the results of both validation procedures and VI states the insights obtained through the experiments.

II. PROBLEM STATEMENT

A. Notation

The following notation is used throughout the paper.

- The Euclidean norm of either a vector or a matrix of real numbers is denoted by $\|\cdot\|^2$.
- Given a series of vectors $u_i \in \mathbb{R}^n$, $\mu_u \in \mathbb{R}^n$ is the mean value of the series calculated as $\frac{1}{N}\sum_{i=1}^{N} u_i$.

B. F/T Sensors Calibration

The strain gauge technology bases its measurements in the changes of the resistance according to small deformations of the material. The sensor is designed such that the resulting deformation in the sensors structure are inside the linear section of the material for the specified range. Because of this, a linear relationship between deformation and forces is assumed. We assume that the model of the sensor is linear and has the following form:

$$w = Cr + o \qquad (1)$$

where $w \in \mathbb{R}^6$ are the wrenches, $C \in \mathbb{R}^{6\times6}$ is the calibration matrix, $r \in \mathbb{R}^6$ are the raw measurements and $o \in \mathbb{R}^6$ is the offset.

Both the calibration matrix C and the offset o are typically unknown and need to be estimated. Assuming that for a series of raw measurements r_i, we have the corresponding wrench applied on the sensor w_i, we can cast the problem of finding the calibration matrix and the offset as a multiple line regression using least squares fitting technique. The calibration matrix estimation can be considered as six different problems in which each row is a separate problem with six independent variables as input and one dependent variable output. For the sake of simplicity we solve all six axis at once. Thus the problem is stated as follows:

$$\arg \min_{C,o} \quad \frac{1}{N}\sum_{i=1}^{N} \|w_i - Cr_i - o\|^2 \qquad (2)$$

Where N is the number of data samples in the dataset. In classical calibration matrix estimation algorithms, the input data (r_i, w_i), $i = 1 \dots N$ are obtained by applying a set of known masses in known locations with the sensor mounted on the workbench. For this reason we will refer to this kind of calibration as *Workbench* calibration.

As discussed in [11], it is typically preferred to estimate offset separately from the calibration matrix, as the offset can typically vary across different experiments due to temperature drift, so the offset is removed from the raw measurements separately, and the calibration problem is reduced to:

$$\arg \min_{C} \quad \frac{1}{N}\sum_{i=1}^{N} \|w_i - Cr_i\|^2 . \qquad (3)$$

III. MODEL BASED IN SITU CALIBRATION METHOD

Once a sensor is mounted in a complex structure such as humanoid robot, its calibration matrix may change due to the internal deformation caused by the mounting screws and other mounting deformations [11]. For this reason we need to *recalibrate* the F/T sensor using a set of *in situ* samples (r_i, w_i), $i = 1 \dots N$ obtained directly on the robot.

If it is known that no external wrench is acting on the limb on which the F/T sensor is mounted, then the expected wrench applied on the sensor can be computed using limb model and the instantaneous limb joints position, velocity and acceleration [14].

A. Centralized offset removal from training in situ datasets

Once the *in situ* calibration data (r_i, w_i), $i = 1 \ldots N$ are available, we need to get rid of the offset, even before estimating the calibration matrix.

In this section, we propose a method to obtain a problem in the form (3), without the need of computing the offset o.

We centralize the data since for a problem of the form of 2, the solution for the optimal calibration matrix C^* and optimal offset o^* is given by

$$o^* = \mu_w - C^* \mu_r. \tag{4}$$

So the form of the problem becomes independent of the offset and can be reduced to:

$$\hat{w}_i = w_i - \mu_w, \qquad \hat{r}_i = r_i - \mu_r, \tag{5}$$

$$\arg\min_{C \in \mathbb{R}^{6 \times 6}} \quad \frac{1}{N} \sum_{i=1}^{N} \left\| \hat{w}_i - C\hat{r}_i \right\|^2. \tag{6}$$

Where $\mu_w \in \mathbb{R}^6$ is the vector of the mean of the wrenches, $\mu_r \in \mathbb{R}^6$ the vector of the mean of the inputs, $\hat{w}_i \in \mathbb{R}^6$ and $\hat{r}_i \in \mathbb{R}^6$ are the *centralized* data. Note that even if in (6) we did not removed explicitly the offset, the resulting optimization problem has the same form of (3), and so for the calibration point of view the proposed algorithm is equivalent to offset removal. A proof for this statement is provided in the appendix VI.

B. Model based in situ calibration matrix estimation

Considering the linear model in (1), a least squares technique is used for performing the linear regression. Assuming the calibration performed on the sensor was correct, we assume the new calibration matrix must not be very different from the matrix obtained using Workbench calibration. To enforce this assumption, we introduce a regularization term to penalize the difference with respect to the Workbench matrix. The new calibration matrix is obtained through the following optimization problem :

$$C^* = \arg\min_{C \in \mathbb{R}^{6 \times 6}} \quad \frac{1}{N} \sum_{i=1}^{N} \left\| \hat{w}_i - C\hat{r}_i \right\|^2 + \lambda \left\| C - C_w \right\|^2 \tag{7}$$

Where $C_w \in \mathbb{R}^{6 \times 6}$ is the *Workbench* calibration matrix provided by the manufacturer, λ is used to decide how much to penalize the regularization term and N is the number of data points in the dataset. The regularization is added in order to try to keep the calibration matrix as close to the Workbench but with an improved performance once the sensor is already mounted on the system.

IV. EXPERIMENTS

Experiments have been performed on the 53 DOF robot iCub. Six custom-made six axes F/T sensors [15], one per ankle, leg and arm, are placed as shown in Fig. 1.

A. Remark on offset removal

While the higher unit resistance and sensitivity of silicon based gauges are definite advantages, their greater sensitivity to temperature variations and tendency to drift are disadvantages in comparison to metallic foil sensors [16]. This plus the effect of hysteresis may result in a different offset value for each experiment, but it is assumed the offset remains constant during the experiment due to the small time frame of each experiment. The effects of drift and hysteresis are currently not considered in the model. This also mean that the offset estimation should be done before every experiment, but this is trivial once the calibration matrix is known.

In the experimental settings, two methods were compared to remove the offset from the estimation problem. The first one is the *centralized offset removal* introduced in this paper, while the second method is the *in situ offset estimation* proposed in [11], where the accelerometers measurements are simulated using the kinematic model of the robot. This method has the advantage that the *real* offset is directly calculated in the raw data and is independent of the estimated calibration matrix. It assumes a constant center of mass which prevents the use of this method in all datasets since this assumption is not always enforced.

In both cases we end up with a modified version of the raw data in which the effect of the offset is removed. With a little abuse of notation we have:

$$\hat{r}_i = \begin{cases} r_i - o_r & \text{in situ offset estimation} \\ r_i - \mu_r & \text{centralized offset removal} \end{cases} \tag{8}$$

$$\hat{w}_i = \begin{cases} w_i & \text{in situ offset estimation} \\ w_i - \mu_w & \text{centralized offset removal} \end{cases} \tag{9}$$

Where $\hat{r}_i$ and $\hat{w}_i$ are the data used to solve the model based in situ calibration problem (7).

B. Training Datasets

We have 3 types of datasets:

- **Grid**: moving the legs in a grid pattern on a fixed pole. The contact is on the waist of the robot.
- **Balancing**: doing a one foot balancing demo. The external contact is the support foot. A video of this demo can be found in [17].
- **Extended Balancing**: doing an extended one foot balancing demo with more widespread leg movements. The contact is on one support foot.
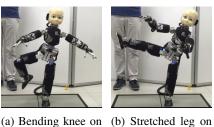
Both the balancing demo and the extended balancing involve more general movements like flexing the legs, reason for which the offset can only be removed using the *centralized offset removal* method.

The following assumptions are valid for all datasets:

- There is only one contact point where external force is applied and its location is known.
- Rigid body inertial parameters are known.
- Relation between raw measurements and F/T values is a linear affine transformation.

(a) Bending knee on left leg support

(b) Stretched leg on left leg support

(c) Moving back to front and sideways

(d) Stretching to the front, side view

(e) Bending knee on right leg support

(f) Streched leg on right leg support

Fig. 2: Images from the extended balancing demo with contact switching

- The offset does not change during the experiment, although it may be different in the other experiments.
- The effects of drift and hysteresis are negligible due to the short time range of the experiments.

The wrenches used as reference are estimated through the model and kinematic measurements using the methods described in [14].

C. Validation procedures

For comparing and validating the results 7 different datasets where used: one balancing experiment, two extended balancing at slow speed, two extended balancing with a faster movement and two grid pattern experiments one with a wider joint range than the other. Most of the datasets were taken on different days. All of them were taken on the same robot with the same sensors, and the sensors were never unmounted from the robot in the time between two experiments.

Two different validation procedures were done to compare the resulting calibration matrices. In the first procedure, we simply test the calibration matrices obtained on each dataset with $\lambda = 0$ against all others including the original calibration matrix provided by the manufacturer, which will be called hence forth as the *Workbench* matrix. This is in order to determine if one experiment was more representative and useful than the others.
For the second validation procedure different calibration matrices are generated with varying values of λ and then are tested on a dataset performing movements similar to the actual use of the robot, in this case an extended balancing dataset with contact switching. They are compared through an estimation of the external forces in the section between the ankle and the hip. This computation is done through the algorithm proposed in [14]. The estimation considers the gravity and, in the ideal case, it should show a value of 0, since during the experiments no external force was applied to the robot in that subchain. The experiment in which it was validated starts with the robot hanging in the air. Then performing the extended balancing demo on both feet one after the other as shown in fig. 2. This is to include many of the behaviours expected form a general use of the robot and see the benefits of the *In situ* calibration. The important restriction kept during the experiment is that the only external force acting on the robot was gravity.
In the first method the best calibration matrix is the one in which the error with respect to the estimated wrenches
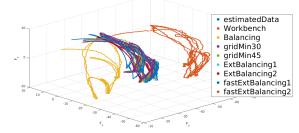

Fig. 3: 3D force comparison among the calibration matrices trained on each dataset against the model estimated forces on the fastExtBal1 dataset.

is lower. To avoid problems with comparing different units, N and Nm, we do the comparison on the error percentage calculated in the following way:

$$e_{d\%} = \frac{w_{ref} - C_d r_{ref}}{w_{ref} - C_w r_{ref}}$$

Where d is the dataset in which the calibration matrix was calculated, ref is the dataset in which the calibration matrix is being tested, $C_d \in \mathbb{R}^{6\times6}$ is the calibration matrix calculated on the d dataset and $e_{d\%}$ is the error percentage of C_d. In this case if an experiment performs worse than the Workbench matrix it is automatically discarded for the second validation procedure.

V. RESULTS

A. First validation procedure

Table I summarizes the errors of all axis of all datasets against all datasets. The rows represent the dataset in which it was tested and the columns the calibration matrix that was used to calculate the error. It can be seen that the calibration matrix obtained from the simple balancing experiment performs worse than those of the Workbench matrix. This is confirmed in figure 3, which as an example of the error of the different calibration matrices on a dataset. All the other calibration matrices give results relatively close to each other and are indeed way better than the results of the Workbench matrix.

Using this procedure the calibration matrix with better results on general is the 2_{nd} extended balancing dataset with the code name of "ExtBal2".
Since each axis can be seen as an independent problem we

TABLE I: Error percentage between calibration matrix and estimated wrenches ($e_{d\%}$) over all datasets.

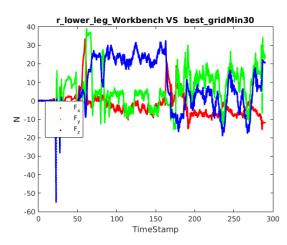| Dataset (ref)	Workbench	Balancing	gridMin30	gridMin45	ExtBal1	ExtBal2	fastExtBal	fastExtBal2
Balancing	100	17.29	110.38	103.37	55.09	57.53	0.4977	0.5813
gridMin30	100	464.82	13.19	18.29	25.13	23.69	0.3311	0.2426
gridMin45	100	532.59	12.94	10.99	22.47	25.42	29.68	25.61
ExtBal1	100	102.50	39.84	30.20	25.88	23.48	34.70	25.81
ExtBal2	100	128.64	33.03	28.02	28.25	26.83	35.26	25.76
fastExtBal	100	107.44	43.51	31.65	28.00	26.14	36.57	26.55
fastExtBal2	100	118.52	33.18	29.80	27.87	24.45	34.94	27.34

Fig. 4: Difference between forces obtained with the Workbench calibration and the best *in situ* calibration matrix

TABLE III: Best calibration matrix for each axis

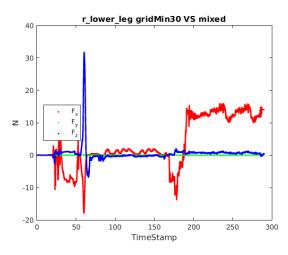| Axis	1_{st} Validation		2_{nd} Validation	
	Dataset	Error %	Dataset	Mean N / Nm
f_x	ExtBal2	28.43	ExtBal1$_{\lambda 10}$	8.13
f_y	fastExtBal	14.30	gridMin30	14.83
f_z	ExtBal1	56.85	gridMin45	13.46
τ_x	ExtBal2	54.62	fastExtBal2$_{\lambda 1.5}$	4.60
τ_y	Workbench	100	Workbench	0.58
τ_z	Workbench	100	fastExtBal2$_{\lambda 10}$	1.88

Fig. 5: Difference between the forces obtained using the best new calibration matrix and the mixed matrix

also considered the calibration matrix which has better results in each axis. The results are shown on Table III.

The results from the first validation procedure highlight how the calibration matrix trained on the normal balancing dataset was found to perform consistently worse then the *Workbench* calibration matrix, and for this reason it was not included in the second validation procedure.

B. Second validation procedure

The λ values used for the second validation procedure are [0.5 1 1.5 2 4 6 8 10]. 41 different calibration matrices where tested. Eight calibration matrices where generated for each valid dataset except the one in which they were tested. The results can be summarized in the table II.

For this procedure the calibration matrix with better results on general is the fixed pole dataset with the code name of "gridMin30". The difference between the magnitude of the forces at each axis between the Workbench and the "grid-Min30" can be seen in figure 4. The mayor improvements are on the f_y and f_x axis.

Since each axis can be seen as an independent problem, it is possible to see a further improvement if we take the best for each axis separately, which we will call "mixed". This comparison can be seen in figure 5. The results are shown in Table III.

The improvement in the measurements was observed when the movement of the robot used to do the *in situ* calibration spans a wide amount of the operational space. In the case of the first validation procedure we where also able to observe that when looking at the axis separately in the

case of the torques the Workbench matrix still out performs the others.It also justifies our choice of the regularization parameter to penalize the difference with respect to the Workbench. In the second validation procedure, it is possible to observe that, removing the offset as suggested in [11] gives calibration matrices that outperform the others in a more general scenario, something that was not reflected during the first validation procedure. This implies that a simple dataset with the robot on the pole moving the legs around is enough to perform a good enough calibration that can outperform datasets obtained using more complex scenarios. It should also be noted that difference in the magnitude of the force obtained with the new calibration matrix is around 25% better than the Workbench. Since this calibration depends on the calibration matrix of two different sensors, the one in the ankle and the one in the hip, part of the magnitude of the force seen in this validation may be due to the fact that the one from the ankle has not been optimized. We expect better results once that sensor is also calibrated *in situ*.

It can be seen that there is more than one optimal λ value

TABLE II: Mean value of error on the external force (N) estimated on the extended balancing dataset using the different calibration matrices with different λ values

Dataset (ref)	0	0.5	1	1.5	2	4	6	8	10
Workbench	31.3111	-	-	-	-	-	-	-	
ExtBal1	-	30.7219	30.7553	30.7218	30.7498	30.7285	30.7670	30.7593	30.7847
ExtBal2	-	33.5694	33.5650	33.5620	33.5504	33.5609	33.5823	33.5533	33.5698
fastExtBal2	-	33.8062	33.8423	33.8398	33.8469	33.8275	33.8646	33.8530	33.8441
gridMin30	-	23.5073	23.5635	23.6338	23.7039	23.9476	24.1988	24.4084	24.6439
gridMin45	-	24.2435	24.2729	24.3017	24.3390	24.4010	24.4761	24.5821	24.6940

depending on the axis. This confirms that the axis are indeed independent problems. Thus, it is possible to use a different solution per axis to obtain an even better final calibration matrix for the F/T sensor.

VI. CONCLUSIONS

In this paper we introduced a new *in situ* calibration technique for six axis F/T sensors that exploit the a-priori knowledge of the inertial parameters model of the robot. We show how the use of such a technique improved the quality of force measurements in the case of the legs of the iCub humanoid robot. Regarding future work we plan to insert the new calibration matrix in the robot and measure the improvements in the performance of the whole body balancing controller [18] as well as finding a set of optimal minimal poses or trajectories to do the calibration.

APPENDIX

Theorem 1. *If C^*, o^* are the solutions to the calibration problem* (2):

$$C^*, o^* = \arg \min_{C,o} \quad \frac{1}{N} \sum_{i=1}^{N} \|w_i - Cr_i - o\|^2. \quad (10)$$

We have that:

$$C^* = \arg \min_{C} \quad \frac{1}{N} \sum_{i=1}^{N} \|\hat{w}_i - C\hat{r}_i\|^2, \quad (11)$$

$$o^* = \mu_w - C^*\mu_r. \quad (12)$$

Proof. Using the definitions of $\hat{w}_i$ and $\hat{r}_i$ we can write the cost function in (2) as:

$$\frac{1}{N} \sum_{i=1}^{N} \|\hat{w}_i - C\hat{r}_i + \mu_w - C\mu_r - o\|^2 =$$

$$= \frac{1}{N} \sum_{i=1}^{N} \|\hat{w}_i - C\hat{r}_i\|^2 + \frac{1}{N} \sum_{i=1}^{N} \|\mu_w - C\mu_r - o\|^2 +$$

$$+ \frac{2}{N} \sum_{i=1}^{N} (\hat{w}_i - C\hat{r}_i)^\top (\mu_w - C\mu_r - o).$$

As $\sum_{i=1}^{N} \hat{w}_i = 0$ and $\sum_{i=1}^{N} \hat{r}_i = 0$ from their definition (5) we get that the third term of the is always equal to zero, and so we have that the calibration problem reduces to:

$$C^*, o^* = \arg \min_{C,o} \quad (\frac{1}{N} \sum_{i=1}^{N} \|\hat{w}_i - C\hat{r}_i\|^2 +$$

$$+ \|\mu_w - C\mu_r - o\|^2)$$

Noting that the minimum of the second term is always 0 for $o = \mu_w - C\mu_r$, $\forall C$, we prove the theorem. $\square$

REFERENCES

[1] P. Watson and S. Drake, "Pedestal and wrist force sensors for automatic assembly," in *Proceedings of the 5th International Symposium on Industrial Robots*, 1975.

[2] D. E. Whitney, "Historical perspective and state of the art in robot force control," *The International Journal of Robotics Research*, vol. 6, no. 1, 1987.

[3] DRC-Teams, "What happened at the DARPA Robotics Challenge?" 2015. [Online]. Available: www.cs.cmu.edu/~cga/drc/events

[4] ATI Industrial Automation, "Six-Axis Force/Torque Transducer Installation and Operation Manual," 2014. [Online]. Available: http://www.webcitation.org/6SGCDRq6M

[5] Weiss Robotics, "KMS 40 Assembly and Operating Manual," 2013. [Online]. Available: http://www.webcitation.org/6SBosGSjQ

[6] A. Tar and G. Cserey, "Development of a low cost 3d optical compliant tactile force sensor," in *Advanced Intelligent Mechatronics (AIM), 2011 IEEE/ASME International Conference on*. IEEE, 2011.

[7] D. B. . H. Wrn, "Techniques for robotic force sensor calibration," in *13th International Workshop on Computer Science and Information Technologies (CSIT2011)*, no. 4(44), 2011.

[8] M. Uchiyama, E. Bayo, and E. Palma-Villalon, "A systematic design procedure to minimize a performance index for robot force sensors," *Journal of Dynamic Systems, Measurement, and Control*, vol. 113, no. 3, 1991.

[9] G. S. Faber, C.-C. Chang, I. Kingma, H. Martin Schepers, S. Herber, P. H. Veltink, and J. T. Dennerlein, "A force plate based method for the calibration of force/torque sensors," *Journal of biomechanics*, vol. 45, no. 7, 2012.

[10] C. M. Oddo, P. Valdastri, L. Beccai, S. Roccella, M. C. Carrozza, and P. Dario, "Investigation on calibration methods for multi-axis, linear and redundant force sensors," *Measurement Science and Technology*, vol. 18, no. 3, 2007.

[11] S. Traversaro, D. Pucci, and F. Nori, "In situ calibration of six-axis force-torque sensors using accelerometer measurements," in *2015 IEEE International Conference on Robotics and Automation (ICRA)*, May 2015.

[12] B. Shimano and B. Roth, "On force sensing information and its use in controlling manipulators," in *Proceedings of the IFAC International Symposium on information-Control Problems in Manufacturing Technology*, 1977.

[13] H. Roozbahani, A. Fakhrizadeh, H. Haario, and H. Handroos, "Novel online re-calibration method for multi-axis force/torque sensor of iter welding/machining robot," *Sensors Journal, IEEE*, vol. 13, no. 11, Nov 2013.

[14] M. Fumagalli, S. Ivaldi, M. Randazzo, L. Natale, G. Metta, G. Sandini, and F. Nori, "Force feedback exploiting tactile and proximal force/torque sensing," *Autonomous Robots*, vol. 33, no. 4, 2012.

[15] M. Fumagalli, M. Randazzo, F. Nori, L. Natale, G. Metta, and G. Sandini, "Exploiting proximal f/t measurements for the icub active compliance," in *Intelligent Robots and Systems (IROS), 2010 IEEE/RSJ International Conference on*, Oct 2010.

[16] OMEGA, "Transactions in measurement and control volume 3, force-related measurements," OMEGA Engineering, INC, Tech. Rep. [Online]. Available: http://www.omega.com/literature/transactions/

[17] [Online]. Available: https://youtu.be/UPOLcE1vwA0

[18] G. Nava, F. Romano, F. Nori, and D. Pucci, "Stability analysis and design of momentum-based controllers for humanoid robots," *Proceedings of the 2016 IEEE/RSJ International Conference on Intelligent Robots and Systems IROS*, Oct 2016.